Selective cyclooxygenase-2 inhibitor NS-398 attenuates myocardial fibrosis in mice after myocardial infarction via Snail signaling pathway

Y.-C. CHI¹, C.-L. SHI², M. ZHOU¹, Y. LIU³, G. ZHANG⁴, S.-A. HOU¹

Abstract. – OBJECTIVE: The role of NS-398 in Snail pathway of myocardial cells in mice after myocardial infarction and its effect on myocardial fibrosis were investigated in this study.

MATERIALS AND METHODS: C57BL/6 mice were selected to establish mouse models of myocardial infarction with permanent ligation of anterior descending branch and sham-operation models without ligation. After successful establishment of models, 30 mice were randomly divided into sham-operation group, myocardial infarction group and drug intervention group. The drug intervention group was treated with intraperitoneal injection of NS-398 (5 mg/kg) at 1 week after modeling for 3 weeks. The survival status of mice after operation was monitored, the cardiac function was detected via echocardiography, the collagen levels in heart tissue pathological sections were detected via Masson staining and Sirius red staining. Moreover, the expressions of Snail and type I collagen levels were detected via immunohistochemistry, and the Snail protein expression level and the activity and expression level of E-cadherin protein were detected via Western blotting.

RESULTS: At 4 weeks after establishment of myocardial infarction model, the fibrosis reaction was obvious, and the cardiac function was decreased, accompanied with Snail activation. The administration of NS-398 for 3 weeks inhibited the Snail activity expression and significantly improved the fibrosis degree after infarction. However, it did not improve the cardiac function. Inhibiting Snail improved the fibrosis reaction after infarction, in which Snail/E-cadherin signaling pathway was involved.

CONCLUSIONS: NS-398 improves the myocardial fibrosis in mice after myocardial infarction through inhibiting the Snail signaling pathway.

Key Words:

NS-398, Fibrosis, Myocardial infarction, Snail signaling pathway.

Introduction

A series of pathophysiological changes after myocardial infarction, such as myocardial necrosis, mechanical stress changes, and neurohumoral activation, affect the process of ventricular remodeling and prognosis of diseases1-3. Myocardial fibrosis is an important process of cardiac remodeling, which leads to deterioration of cardiac function, reduces the life quality of patients, and results in poor prognosis and increased mortality rate⁴. At present, the research on the mechanism of cardiac fibrosis has focused on the neurohumoral factors, cytokines, inflammatory responses, etc. Latest studies have shown that extracellular matrix deposition is an important mechanism leading to the organ fibrosis^{5,6}. Fibrous matrix deposition promotes the cardiomyocyte hypertrophy and sclerosis, and further aggravates heart failure; besides, it also increases the risk of malignant arrhythmias⁷. The research on the mechanisms of the self-repair and scar formation in myocardial infarction area, as the source of a large number of cardiac fibroblasts after myocardial injury, is gradually carried out. At present, the clinical effect of anti-fibrosis treatment remains unclear; therefore, further exploring the mechanisms of occurrence and development of cardiac fibrosis from multiple perspectives and searching the target of controlling cardiac remodeling are of great significance. Epithelial-mesenchymal transition (EMT) refers to the changes in the structure and function of epithelial cells, loss of epithelial phenotype and polarity, and increased migration capacity during the normal development process of the body under the stimulation of various physiological and pathological conditions, further differentiating

¹Intensive Care Unit, People's Hospital of Rizhao, Rizhao, China

²Department of Neurosurgery, People's Hospital of Rizhao, Rizhao, China

³Department of Surgery, People's Hospital of Zhangqiu District, Jinan, China

⁴Department of Obstetrics, People's Hospital of Zhangqiu District, Jinan, China

into mesenchymal cells. Previous studies have shown that EMT is an important mechanism of organ damage repair and fibrosis occurrence and development8. EMT signal activates and regulates pathophysiological processes, including scar formation, liver, kidney, lung and peritoneal fibrosis. It has been confirmed in *in vitro* cell culture and animal model experiments that the zinc finger protein transcription factor Snail is involved in the process of organ fibrosis^{9,10}. Recently, studies have found that Snail is activated during fibrosis process in mice and participates in cardiac fibrosis in mice after myocardial infarction¹¹. The selective cyclooxygenase-2 (COX-2) inhibitor NS-398 can effectively inhibit the proliferation of a variety of tumor cells and induce the apoptosis of tumor cells^{12,13}. The abnormal expression of Snail plays an important role in the invasion and metastasis of tumor cells, and the up-regulation of its expression can induce the EMT and tumor formation and make cells invasive¹⁴. Studies have found that NS-398 can regulate the expression of E-cadherin by regulating Snail, thereby affecting the occurrence, invasion and metastasis of tumor cells¹⁵. However, there is no report on whether NS-398 can improve the myocardial fibrosis through regulating the Snail pathway of myocardial cells yet. Therefore, the role of NS-398 in Snail pathway of myocardial cells in mice after myocardial infarction and its effect on myocardial fibrosis were investigated in this study.

Materials and Methods

Laboratory Animal and Myocardial Infarction Model

Specific pathogen-free (SPF) C57BL/6 male mice aged 8-10 weeks selected in this experiment were provided by the Animal Center of People's Hospital of Rizhao (Rizhao, China). The animal experiments were approved by the Ethics Committee of the People's Hospital of Rizhao. Mice were weighed and anesthetized via intraperitoneal injection of tribromoethanol solution [(320±40) mg/kg, prepared at a concentration of 20 mg/mL using normal saline according to the body weight. After the anesthesia took effect, tracheal intubation was performed under direct vision, and the ventilator was turned on and connected. The left chest of the mouse was disinfected using 75% alcohol, and the chest was opened from the 3rd-4th intercostal spaces. After that, the pericardium and its surrounding tissues were separated to expose the heart.

The left anterior descending branch was carefully observed and positioned, and blood vessels were ligated with 8-0 needle thread at about 2-3 mm below the edge of left auricle. After knotting, distal left ventricular myocardium turned pale, and it could be used as evidence of accurate ligation. The thorax was slightly squeezed to discharge all the pneumatosis and then sutured layer by layer. The incision and surrounding skin were disinfected again using 75% alcohol, and resuscitated on the electric blanket. For mice in sham-operation group, after the left anterior descending was positioned, the blood vessels were sutured with 8-0 needle thread without knotting. The remaining operations were the same as those in operation group.

Drug Intervention

NS-398 dimethylsulfoxide (DMSO) solution was prepared. At 1 week after modeling, mice with myocardial infarction were randomly selected and intraperitoneally injected with NS-398 (5 mg/kg) for 21 consecutive days (once/day). The same amount of DMSO solution without drugs was given to mice in control group.

Echocardiography

Mice were taken, fixed and anesthetized via 2.5% isoflurane. Echocardiography was performed using the Vev0770 high-resolution system ultrasonic apparatus (probe frequency: 40-MHz, respiratory minute volume: 704). First, the parasternal left ventricular long-axis section was explored, and then the probe was rotated for 90° clockwise to get the parasternal left ventricular short-axis section. The probe position was adjusted to the horizontal section of papillary muscle with the sampling line perpendicular to the posterior wall of left ventricle. Then, the M-mode ultrasound was selected, followed by measurement, recording, and saving of detection information.

Pathological Sections

Specimens were pre-cooled in a refrigerator at -20°C, the microtome was turned on and the section thickness was set [5 μ m in hematoxylin and eosin (HE) staining and Masson trichrome staining; 8 μ m in Sirius red staining] to cut the desired number of sections. These were placed at 45°C for water bath; the specimen sections were salvaged with a clean glass slide and dried on a baking machine at 60°C for 1 h. Sections were soaked in xylene, dehydrated with gradient alcohol, and finally soaked in distilled water for standby application.

HE Staining

Sections were washed with distilled water and stained in a hematoxylin dye vat for 5 min. After being washed again with distilled water for 5 min, sections were stained in eosin dye for 5-8 s, and immediately placed in distilled water to terminate the staining, followed by neutral resin glue sealing, observation, and photography under a light microscope.

Masson Staining

According to the instructions of kit (Nanjing Senbeijia Biological Technology Co., Ltd. Nanjing, China), after treatment, sections were stained via the same amount of hematoxylin dye and ferric chloride aqueous solution for 5-10 min, followed by differentiation via hydrochloric acid alcohol, and back to blue via ammonia solution. Next, sections were stained by ponceau acid fuchsin dye for 5-10 min, and by phosphomolybdic acid aqueous solution for 1-2 min, followed by washing. Sections were stained by aniline blue dye for 1-2 min and then observed under the light microscope.

Sirius Red Staining

According to the instructions of kit (Nanjing Senbeijia Biological Technology Co., Ltd. Nanjing, China), sections were stained by Sirius red dye for 1 h. After washing, Mayer hematoxylin was used to re-stain the nuclei for 1 min and then for morphology observation.

Immunohistochemistry

After antigen retrieval of sections, 3% hydrogen peroxide solution was added dropwise to block the activity of endogenous peroxidase. Goat serum was added dropwise to seal the sections for 30 min. Then, primary antibody was added dropwise into the sections, while the blank antibody diluent was used as negative control. All sections were placed in a wet box and incubated at 4°C overnight. Biotin-labeled secondary antibody was added dropwise to seal the sections for 30 min, and then 3,3'-diaminobenzidine (DAB) developing solution was added, followed by microscopy and photography.

Immunofluorescence

After dehydration and antigen retrieval of sections, primary antibody was added into the sections at 4°C overnight. The fluorescence-labeled secondary antibody was used to incubate sections at room temperature for half an hour. After 50%

glycerol sealing, sections were observed under a fluorescence microscope.

Western Blotting

Tissues were taken to extract total proteins. According to instructions of the kit (Beyotime, Shanghai, China), standard protein gradient solution was prepared, and the protein concentration of each sample was measured and quantified using the bicinchoninic acid (BCA) method. After sodium dodecyl sulfonate gel electrophoresis, proteins were transferred onto polyvinylidene difluoride (PVDF) membrane. The target protein primary antibody was incubated at 4°C overnight. On the second day, chemiluminescence liquid was used for color development after incubation of the secondary antibody, and the membrane was exposed and developed in a chemiluminescence imager.

Statistical Analysis

Statistical Product and Service Solutions (SPSS) 19.0 software (IBM, Armonk, NY, USA) was used for the statistical analysis of data. Student's t-test was used for analysis of means. Bonferroni correction method or Tamhane's T2 correction method was used for the intergroup analysis of variance. Data were presented as mean \pm standard deviation. p<0.05 suggested that the difference was statistically significant.

Results

NS-398 Did Not Significantly Improve the Cardiac Function in Mice After Myocardial Infarction

The heart rate of mice in myocardial infarction group was significantly increased compared with that in sham-operation group. At the same time, in myocardial infarction group, the left ventricular anterior wall thickness was significantly reduced, the left ventricular cavity was enlarged, the cardiac function was deteriorated, and the left ventricular ejection fraction and left ventricular shortening fraction were significantly decreased compared with those in sham-operation group. After drug intervention, echocardiography showed that the left ventricular cavity was smaller and the left ventricular anterior wall thickness was increased in sham-operation group compared with those in myocardial infarction group, but the cardiac function had no significant improvement.

The heart and lung weight of mice in myocardial infarction group was significantly increased compared with that in sham-operation group, showing tissue damage repair and inflammatory infiltration. The heart weight/body weight ratio still had a clear difference after the heart and lung weight and body weight were calibrated due to the different growth status of mice. The heart and lung weight of mice in drug intervention group were larger than that in sham-operation group, but there were no statistically significant differences compared with those in myocardial infarction group. No statistically significant differences were found between two groups after the body weight was calibrated (Figure 1).

NS-398 Improved the Myocardial Fibrosis in Mice After Myocardial Infarction

Results of HE staining showed that compared with those in sham-operation group, the myocardial tissues around the infarct region were arranged in disorder with necrosis and infiltration of a large number of inflammatory cells in myocardial infarction group, showing damage and injury

repair. The myocardial necrosis and inflammatory infiltration in drug intervention group were improved compared with those in myocardial infarction group (Figure 2A).

Masson staining revealed that myocardial infarction could be seen under a low-power microscope; the scar in myocardial infarction group accounted for more than 40% of the left ventricular myocardium, while the scar area in drug intervention group was smaller than that in myocardial infarction group. Under a high-power microscope, collagen infiltration could be observed around the infarct region; there was no or only a very small amount of blue-stained collagen in myocardium in sham-operation group, while the number of collagen was significantly increased in myocardial infarction group, infiltrating between myocardial cells in a cross-linked way. After drug intervention, the number of collagen tissues was significantly reduced, and the infiltration status among myocardial tissues was significantly alleviated (Figure 2B).

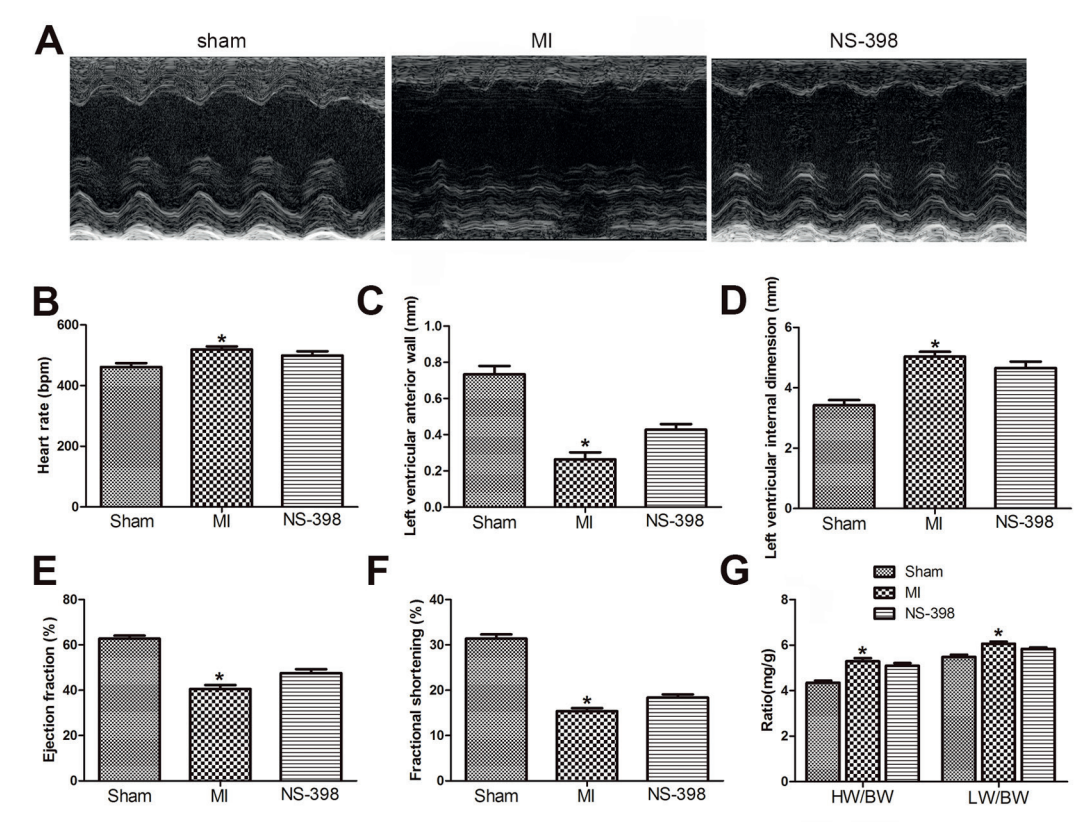


Figure 1. The effects of NS-398 on the cardiac function in mice after myocardial infarction. (A) Representative images of echocardiography. (B) Analysis of heart rate. (C) Analysis of left ventricular anterior wall thickness. (D) Analysis of left ventricular internal dimension. (E) Analysis of left ventricular ejection fraction. (F) Analysis of left ventricular fractional shortening. (G) Analysis of the ratio of heart weight/body weight (HW/BW) and lung weight/body weight (LW/BW). *p<0.05 vs. Sham group.

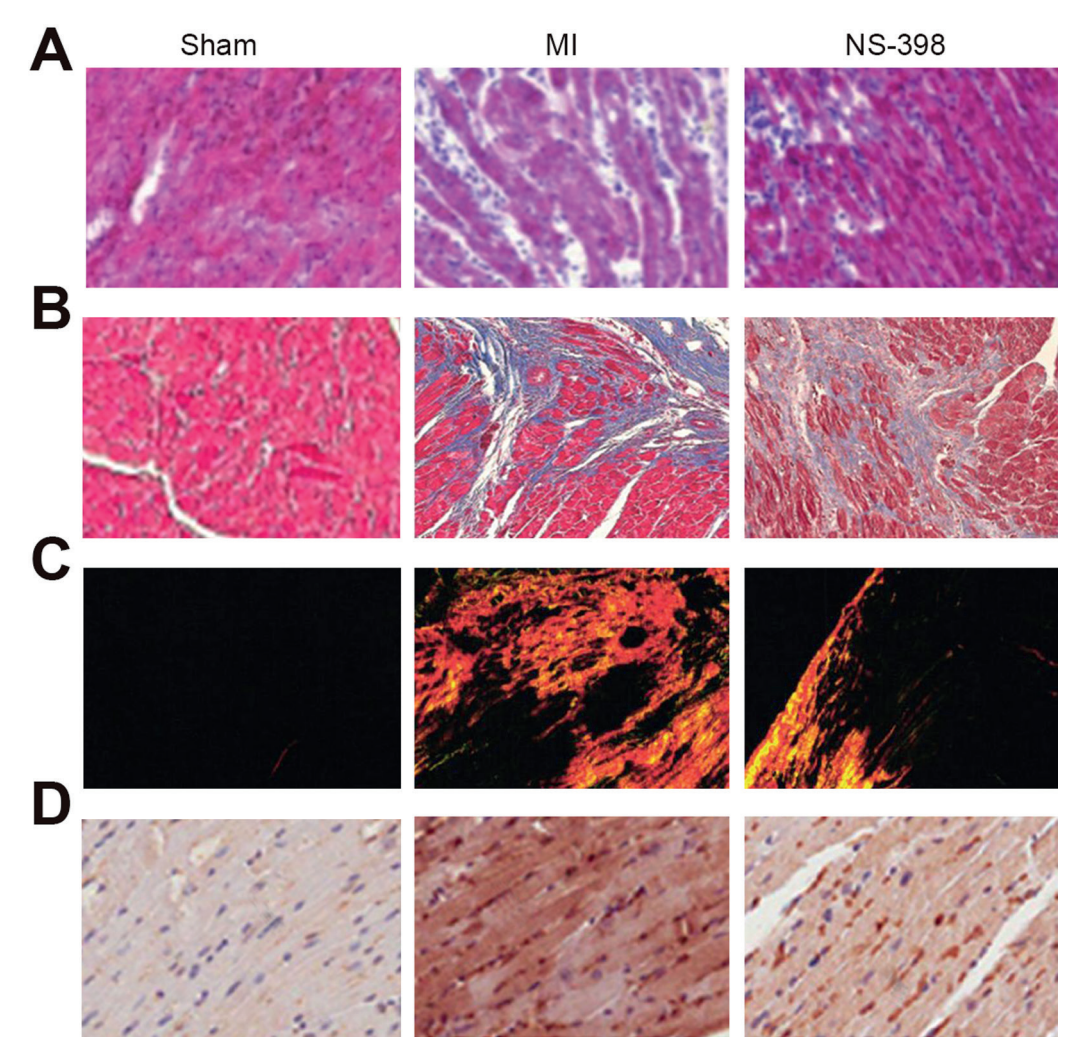


Figure 2. NS-398 improved the myocardial fibrosis in mice after myocardial infarction. (A) Representative images of HE staining. (B) Representative images of Masson staining. (C) Representative images of Sirius staining. (D) Representative images of immunohistochemistry of collagen I.

Sirius red staining showed that only a small number of fibrous tissues could be detected in sham-operation group, while the number of collagen fibers was increased significantly in myocardial infarction group, infiltrating in normal myocardial tissues. Both type I and type III collagen fibers were visible. The numbers of type I and type III collagen fibers in drug intervention group were significantly decreased, and the infiltration state was significantly improved (Figure 2C).

Immunohistochemical results revealed that the expression level of type I collagen in peripheral area of myocardial infarction was increased in myocardial infarction group, compared with that in sham-operation group, showing brown and deep staining in cytoplasm and among cells. After drug intervention, the expression of type I collagen was significantly inhibited, which had a statistically significant difference compared with that in myocardial infarction group (Figure 2D).

NS-398 Inhibited the Snail Expression in Mice After Myocardial Infarction

Immunohistochemical staining of histopathological sections showed that the Snail expression in myocardium around the infarct region was significantly increased after myocardial infarction, showing an activated state. However, the Snail activity around the infarct region was significantly inhibited after drug intervention. Western blotting of tissue samples also showed the same trends (Figure 3).

NS-398 Up-regulated the Expression of Snail Downstream Protein E-cadherin

Immunofluorescence staining of histopathological sections revealed that E-cadherin was expressed in epicardium in sham-operation group, while it was not expressed in epicardium around the infarct region after myocardial infarction. After drug intervention, the expression of E-cadherin could be seen around the infarct region. Results of Western blotting further illustrated the above trends (Figure 4).

Discussion

Under pathological conditions, a large number of interstitial fibroblasts proliferate with excessive deposition of extracellular matrix, so that the collagen content, concentration, and volume fraction per unit mass were significantly higher than normal¹⁶. Such pathological manifestations lead to pathological cardiac hypertrophy and increased hardness, resulting in myocardial diastolic and systolic dysfunction, which are considered to be an important link in the occurrence and development of a variety of cardiovascular diseases. In mouse models of myocardial infarction, reactive fibrosis proliferation could be found around the infarct region with the prolongation of time.

Fibroblasts differentiate under the ischemia-hypoxia conditions and further secrete collagen fibers and other proteins and cytokines, which are involved in the repair process after infarction. In this experiment, in case of the moderate infarct area, the left ventricular anterior wall of mice was thinner, the ventricular cavity was enlarged and the ventricular systolic function declined during 4 weeks, and some mice died for heart failure. The detection of heart in mice also showed myocardial necrosis around the infarct area and disordered cell structure with inflammatory cell infiltration; moreover, due to the differentiation and secretion of myofibroblasts, the content of type I collagen fibers and type III collagen fibers was significantly increased, reflecting the degree and progression of fibrosis. EMT is involved in the organ fibrosis process, which has multiple regulatory transcription factors¹⁷. Snail has been shown to be involved in the regulation of organ fibrosis. E-cadherin is a direct downstream target of Snail. Snail converts epithelial cells to mesenchymal cells by directly inhibiting the expression of E-cadherin and decreasing cell adhesion¹⁸. In this experiment, the expression of Snail in myocardium of mice after myocardial infarction was significantly increased, but the expression of its downstream protein E-cadherin was decreased, indicating that Snail/E-cadherin signaling path-

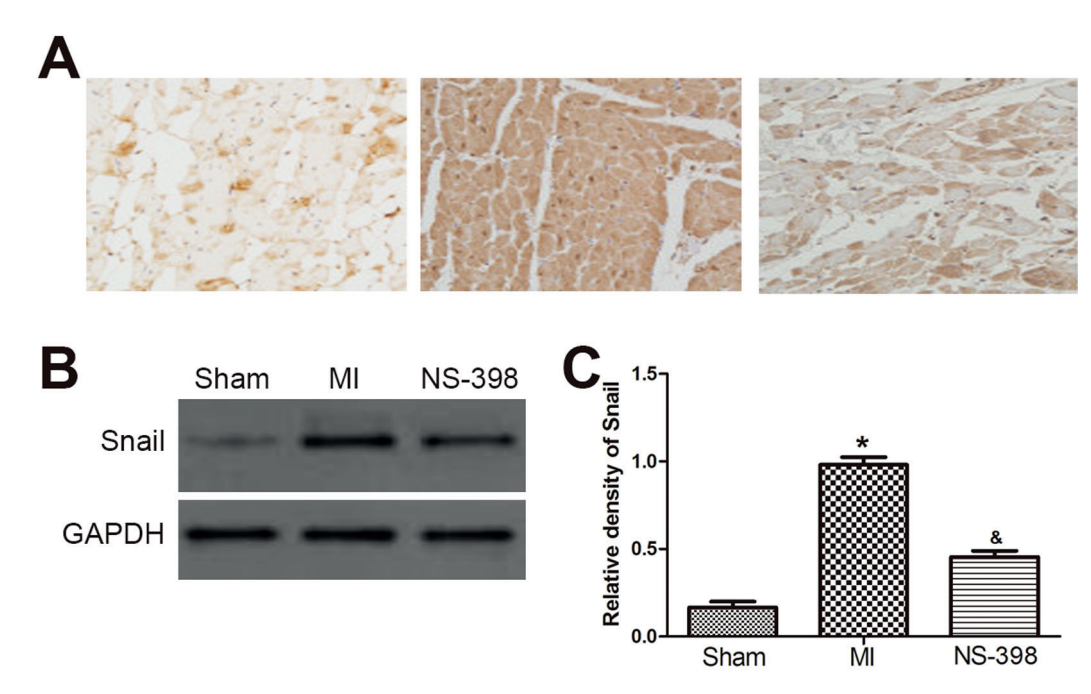


Figure 3. NS-398 inhibited the Snail expression in mice after myocardial infarction. **(A)** Representative images of immunohistochemistry of Snail. **(B)** Western blots analysis reveals the expression of Snail. **(C)** Semi-quantitative analysis of Snail. *p<0.05 vs. Sham group, p<0.05 vs. MI group.

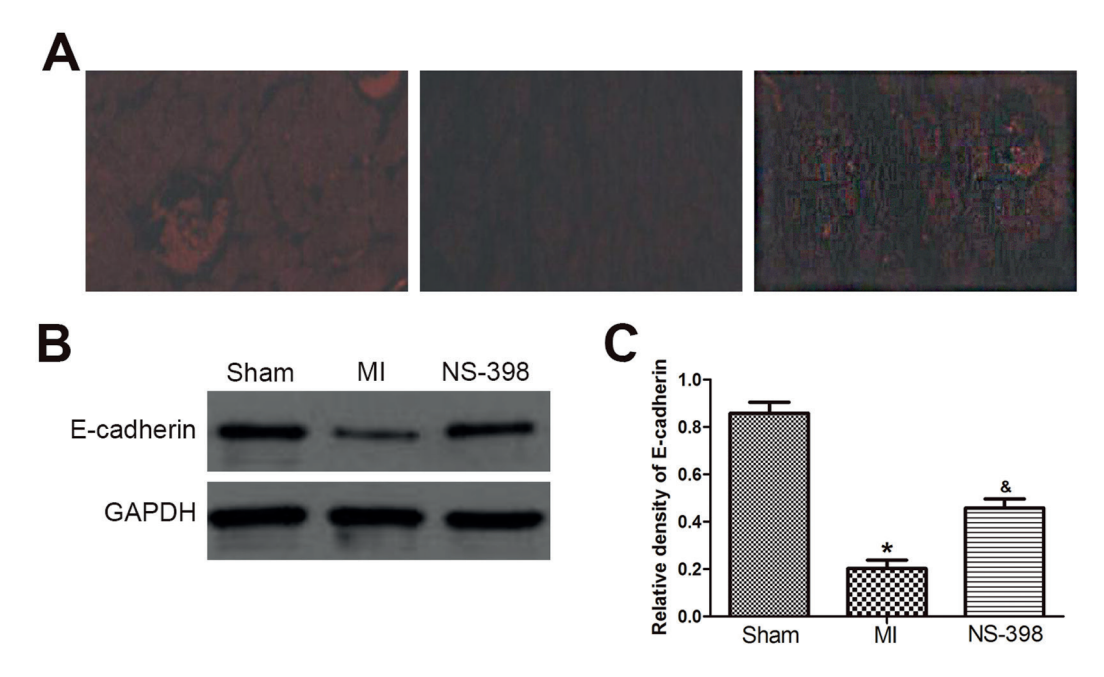


Figure 4. NS-398 up-regulated the expression of Snail downstream protein E-cadherin. (A) Representative images of immunohistochemistry of E-cadherin. (B) Western blots analysis reveals the expression of E-cadherin. (C) Semi-quantitative analysis of E-cadherin. *p<0.05 vs. Sham group, p<0.05 vs. MI group.

way is activated and involved in the pathological process of fibrous repair after infarction. In this experiment, drug intervention was started at 1 week after infarction. After 3 weeks of successive administration, immunohistochemical assay and Western blotting showed that the expression of Snail was significantly inhibited, and no experimental mice died. Pathological detection showed that the degree of fibrosis was significantly reduced, and the secretion of type I collagen fibers and type III collagen fibers were significantly decreased. It is well-known that type I collagen fibers are thick and stiff, while type III collagen fibers have a fine structure and large elastic contraction, seriously affecting the cardiac systolic and diastolic functions¹⁹. The generations of type I and type III collagen fibers have effects on cardiac function and compliance. However, it is interesting that although echocardiography showed that the left ventricular anterior wall was thickened, ventricular cavity was reduced and ventricular ejection fraction was increased after inhibition of Snail and alleviation of myocardial fibrosis after infarction; these improvement effects had no statistically significant differences. The possible reason may be that animal models of myocardial infarction were established in this experiment, but the infarct area was not particularly large, accounting for about 50% of the entire left ventricle,

so it did not cause extremely serious impact on cardiac function, and the improvement in cardiac function in drug intervention group did not show a significant difference in the injury repair process. Furthermore, the pathological fibrosis repair after myocardial infarction is a sustained state of over-activation. With the development of pathological process of myocardial infarction, the fibrosis progressively aggravates and the cardiac function gradually deteriorates. In this experiment, the experimental intervention was terminated at 4 weeks. Although the secretion of collagen fibers and the conversion of collagen type were significantly inhibited, 21-day drug intervention might not be sufficient to significantly improve the cardiac function. However, it is reasonable to assume that with the prolongation of action time, the cardiac function of mice in drug intervention group will be significantly improved compared with that in experimental group, due to the inhibition of pathological fibrosis reaction.

Conclusions

At 4 weeks after establishment of myocardial infarction model, the fibrosis reaction was obvious, and the cardiac function was decreased, accompanied by Snail activation. The admini-

stration of NS-398 for 3 weeks inhibited the Snail activity expression and significantly improved the fibrosis degree after infarction; however, it did not improve the cardiac function. Inhibiting Snail improved the fibrosis reaction after infarction, in which Snail/E-cadherin signaling pathway was involved. In sum, NS-398 improves the myocardial fibrosis in mice after myocardial infarction through inhibiting the Snail signaling pathway.

Conflict of Interest

The Authors declare that they have no conflict of interest.

References

- HENNING RJ, KHAN A, JIMENEZ E. Chitosan hydrogels significantly limit left ventricular infarction and remodeling and preserve myocardial contractility. J Surg Res 2016; 201: 490-497.
- TAKANO H, HASEGAWA H, NAGAI T, KOMURO I. Implication of cardiac remodeling in heart failure: Mechanisms and therapeutic strategies. Intern Med 2003; 42: 465-469.
- Ruping Q, Kuken B, Huang Y, Sun J, Azhati A. Effection of myocardial cell/collagen compound on ventricular electrophysiology in rats with myocardial infarction. Eur Rev Med Pharmacol Sci 2016; 20: 2357-2362.
- 4) LIU T, SONG D, DONG J, ZHU P, LIU J, LIU W, MA X, ZHAO L, LING S. Current understanding of the pathophysiology of myocardial fibrosis and its quantitative assessment in heart failure. Front Physiol 2017; 8: 238.
- DUVAL F, MORENO-CUEVAS JE, GONZALEZ-GARZA MT, RODRIGUEZ-MONTALVO C, CRUZ-VEGA DE. Protective mechanisms of medicinal plants targeting hepatic stellate cell activation and extracellular matrix deposition in liver fibrosis. Chin Med 2014; 9: 27.
- Luo Y, Wang Y, Shu Y, Lu Q, Xiao R. Epigenetic mechanisms: an emerging role in pathogenesis and its therapeutic potential in systemic sclerosis. Int J Biochem Cell Biol 2015; 67: 92-100.
- 7) ARCARO A, PIROZZI F, ANGELINI A, CHIMENTI C, CROTTI L, GIORDANO C, MANCARDI D, TORELLA D, TOCCHETTI CG. Novel perspectives in redox biology and pathophysiology of failing myocytes: modulation of the intramyocardial redox milieu for therapeutic interventions--a review article from the working group of cardiac cell biology, Italian Society of Cardiology. Oxid Med Cell Longev 2016; 2016: 6353469.
- Stone RC, Pastar I, OJEH N, CHEN V, LIU S, GARZON KI, TOMIC-CANIC M. Epithelial-mesenchymal transition in tissue repair and fibrosis. Cell Tissue Res 2016; 365: 495-506.
- Yang G, Zhao Z, Zhang X, Wu A, Huang Y, Miao Y, Yang M. Effect of berberine on the renal tubular

- epithelial-to-mesenchymal transition by inhibition of the Notch/snail pathway in diabetic nephropathy model KKAy mice. Drug Des Devel Ther 2017; 11: 1065-1079.
- 10) Zou J, Liu Y, Li B, Zheng Z, Ke X, Hao Y, Li X, Li X, Liu F, Zhang Z. Autophagy attenuates endothe-lial-to-mesenchymal transition by promoting Snail degradation in human cardiac microvascular endothelial cells. Biosci Rep 2017; 37. pii: BSR20171049.
- LIU Y, DU J, ZHANG J, WENG M, LI X, PU D, GAO L, DENG S, XIA S, SHE Q. Snail1 is involved in de novo cardiac fibrosis after myocardial infarction in mice. Acta Biochim Biophys Sin (Shanghai) 2012; 44: 902-910.
- 12) PANDEY VK, AMIN PJ, SHANKAR BS. COX-2 inhibitor prevents tumor induced down regulation of classical DC lineage specific transcription factor Zbtb46 resulting in immunocompetent DC and decreased tumor burden. Immunol Lett 2017; 184: 23-33.
- 13) LEMAY R, LEPAGE M, TREMBLAY L, THERRIAULT H, CHAREST G, PAQUETTE B. Tumor cell invasion induced by radiation in Balb/C mouse is prevented by the cox-2 inhibitor NS-398. Radiat Res 2017 Sep 28. doi: 10.1667/RR14716.1. [Epub ahead of print]
- 14) ALKATOUT I, HUBNER F, WENNERS A, HEDDERICH J, WIEDDERMANN M, SANCHEZ C, ROCKEN C, MATHIAK M, MAASS N, KLAPPER W. In situ localization of tumor cells associated with the epithelial-mesenchymal transition marker Snail and the prognostic impact of lymphocytes in the tumor microenvironment in invasive ductal breast cancer. Exp Mol Pathol 2017; 102: 268-275.
- 15) FUJII R, IMANISHI Y, SHIBATA K, SAKAI N, SAKAMOTO K, SHIGETOMI S, HABU N, OTSUKA K, SATO Y, WATANABE Y, OZAWA H, TOMITA T, KAMEYAMA K, FUJII M, OGAWA K. Restoration of E-cadherin expression by selective Cox-2 inhibition and the clinical relevance of the epithelial-to-mesenchymal transition in head and neck squamous cell carcinoma. J Exp Clin Cancer Res 2014; 33: 40.
- 16) ZHANG WQ, YANG CY, LI SM, LIU M, DING M, LIU GH, YANG P. Lipopolysaccharide induced activin A-follistatin imbalance affects cardiac fibrosis. Chin Med J (Engl) 2012; 125: 2205-2212.
- 17) Kajiyama H, Shibata K, Terauchi M, Yamashita M, Ino K, Nawa A, Kikkawa F. Chemoresistance to paclitaxel induces epithelial-mesenchymal transition and enhances metastatic potential for epithelial ovarian carcinoma cells. Int J Oncol 2007; 31: 277-283.
- 18) Yang HW, Lee SA, Shin JM, Park IH, Lee HM. Glucocorticoids ameliorate TGF-beta1-mediated epithelial-to-mesenchymal transition of airway epithelium through MAPK and Snail/Slug signaling pathways. Sci Rep 2017; 7: 3486.
- 19) Kwon WY, Cha HN, Heo JY, Choi JH, Jang BI, Lee IK, Park SY. Interleukin-10 deficiency aggravates angiotensin II-induced cardiac remodeling in mice. Life Sci 2016; 146: 214-221.